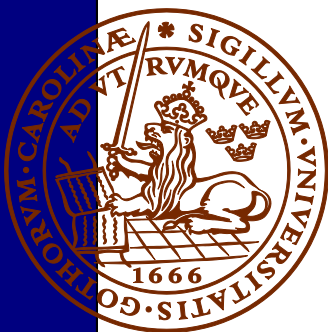


New geochronological constraints on the Klipriviersberg Group: defining a new Neoproterozoic large igneous province on the Kaapvaal Craton, South Africa

Joan Stamsnijder

Dissertations in Geology at Lund University,
Master's thesis, no 524
(45 hp/ECTS credits)



Department of Geology
Lund University
2017

New geochronological constraints on the Klipriviersberg Group: defining a new Neoproterozoic large igneous province on the Kaapvaal Craton, South Africa

Master's thesis
Joan Stamsnijder

Department of Geology
Lund University
2017

Contents

1 Introduction	7
2 Geological setting of the central Kaapvaal Craton	7
3 Samples for U–Pb geochronology	9
4 Analytical protocols	11
4.1 Sample preparation	11
4.2 ID-TIMS	11
4.3 LA-ICP-MS	11
5 Results	12
6 Discussion	14
6.1 LA-ICP-MS and ID-TIMS comparison on baddeleyite	14
6.2 Stratigraphy of the Neoproterozoic Ventersdorp Supergroup and its equivalents	15
7 Implications	17
8 Conclusions	19
9 Acknowledgements	19
10 References	19

Cover Picture: Magnification of baddeleyite, by Prof. Mike Hamilton from the University of Toronto.

New geochronological constraints on the Klipriviersberg Group: defining a new Neoproterozoic large igneous province on the Kaapvaal Craton, South Africa

JOAEN STAMSNIJDER

Stamsnijder, J., 2017: New geochronological constraints on the Klipriviersberg Group: defining a new Neoproterozoic large igneous province on the Kaapvaal Craton, South Africa. *Dissertations in Geology at Lund University*, No. 524, 21pp. 45 hp (45 ECTS credits).

Abstract: In recent years, there has been a significant improvement in our ability to determine the ages of extensive short-lived magmatic events (large igneous provinces) dominated by rocks of mafic (silica-poor) compositions. This has been aided by targeting the magmatic feeders to these large igneous provinces (e.g., dykes and sills), which often host trace amounts of datable zirconium minerals such as baddeleyite and zircon. These age determinations are of great importance for unravelling the geological history and paleogeography of our planet. The Kaapvaal Craton in southern Africa hosts a rich and pristine geological history with many geological units and events in need of better age constraints. One is the Neoproterozoic Ventersdorp Supergroup, with the Klipriviersberg Group, and underlying successions of the Meso- to Neoproterozoic Witwatersrand Supergroup, of which the latter is world-wide known for its association with gold findings. By extracting baddeleyite from intrusive mafic sills from the Witwatersrand sediments, we can obtain critical age constraints for these successions using U–Pb geochronology on baddeleyite. Here we show that feeders to the Klipriviersberg Group are 2787 ± 2 Ma using ID-TIMS and complementary LA-ICP-MS on baddeleyite from two mafic sills. This age makes the Klipriviersberg Group magmatic event almost 80 Myr older than previously thought, and is in agreement with several indirect studies which have suggested a similar age in Ventersdorp Supergroup temporally equivalent basins. Our results imply that there is a significant time gap in the Ventersdorp Supergroup between the deposition of the Klipriviersberg Group and the Platberg Group, and is associated with craton-wide mafic and felsic magmatism. This conclusion implies that the deposition of the Witwatersrand Supergroup ceased before 2787 ± 2 Ma, which is when the eruption of the Klipriviersberg Group basalts commenced. Our results define a new large igneous province on the Kaapvaal Craton, and redefine the timing of both the beginning of Ventersdorp and termination of Witwatersrand supergroups. This new timing indicates that world class gold-bearing conglomerates within the Witwatersrand succession were deposited before 2787 ± 2 Ma.

Keywords: U–Pb geochronology, ID-TIMS, LA-ICP-MS, baddeleyite, Klipriviersberg Group, LIP.

Supervisor: Prof. Ulf Söderlund,

Co-supervisors: Dr. Ashley Gumsley and Dr. Tomas Naeraa.

Subject: Bedrock Geology

*Joan Stamsnijder, Department of Geology, Lund University, Sölvegatan 12, SE-223 62 Lund, Sweden.
E-mail: joan.stamsnijder@gmail.com*

Åldersbestämning av mafiska intrusivbergarter tillhörande Klipriviersberg flodbasalter: omdefinition av en Neoarkeisk vulkanprovins på Kaapvaalkratonen, Sydafrika

JOAEN STAMSNIJDER

Stamsnijder, J., 2017: Åldersbestämning av mafiska intrusivbergarter tillhörande Klipriviersberg flodbasalter: omdefinition av en Neoarkeisk vulkanprovins på Kaapvaalkratonen, Sydafrika. *Examensarbeten i geologi vid Lunds Universitet*, No. 524, 21pp. 45 hp.

Sammanfattning: De senaste åren har det skett avsevärda tekniska och analytiska förbättringar inom radiometrisk metod för åldersbestämning av omfattande men kortlivade magmatiska händelser (s.k. "Large Igneous Provinces"), vilka domineras av bergarter med mafiska (kiselfattiga) sammansättningar. Detta har främjats av att man har riktat in sig på magmatiska gångbergarter (diabaser) som utgör matargångar till stora vulkanprovinser, eftersom diabasgångar ofta innehåller zirkoniummineral såsom baddeleyit och zirkon, vilka kan dateras med hög precision. Åldersbestämningar har stor betydelse för att reda ut jordens geologiska historia och paleogeografi. Kaapvaalkratonen i södra Afrika har en omfattande och rik geologisk historia, och ett stort antal geologiska enheter och händelser som ännu inte åldersbestämts. En av dessa enheter är den Neoarkeiska Ventersdorp Supergruppen, som innefattar Klipriviersberg gruppen, och de underliggande guldbärande sedimentära Meso- till Neoarkeiska Witwatersrand Supergrupp-successioner. Genom att extrahera och analysera baddeleyit från intrusiva mafiska lagergångar i Witwatersrand-sedimenten, kan vi med hjälp av U-Pb geokronologi bedöma åldern på de sedimentära successionerna. Med hjälp av ID-TIMS samt kompletterande LA-ICP-MS visar detta arbete att baddeleyit från magmatiska lagergångar tillhörande Klipriviersberg Gruppen har en ålder på 2787 ± 2 Ma. Detta innebär att Klipriviersberg Gruppen är uppemot 80 Ma äldre vad man tidigare trott. Resultaten antyder att det finns ett signifikant tidsintervall i Ventersdorp Supergruppen, mellan depositionen av Klipriviersberg Gruppen och Platberg Gruppen, vilken är associerad med omfattande mafiskt och felsisk magmatism. Denna slutsats innebär att depositionen av Witwatersrand Supergruppen upphörde innan 2787 ± 2 Ma, vid tiden då eruptionen av Klipriviersberg Gruppen inleddes. Dessa nya resultat definierar en ny vulkansk provins (Large Igneous Province) på Kaapvaalkratonen, och omdefinierar tiden för såväl början av Ventersdorp och avslutningen på Witwatersrand supergrupperna. Den nya åldern innebär att guldbärande konglomerat från Witwatersrand successionerna deponerades innan 2787 ± 2 Ma.

Nyckelord: U-Pb geokronologi, ID-TIMS, LA-ICP-MS, baddeleyit, Klipriviersberg, flodbasalt.

Handledare: Prof. Ulf Söderlund,

Bihandledare: Dr. Ashley Gumsley and Dr. Tomas Naeraa.

Ämnesområde: Berggrundsgeologi

*Joaen Stamsnijder, Geologiska institutionen, Lunds Universitet, Sölvegatan 12, 223 62 Lund, Sverige.
E-post: joaen.stamsnijder@gmail.com*

1 Introduction

The Kaapvaal Craton, situated in southern Africa, hosts a rich and pristine geological history. It has undergone a long and complex history of magmatic events, starting as early as in the Paleoproterozoic. Common igneous intrusions comprise carbonatite and alkali rocks, and mafic and ultramafic rocks, as well as granitoid rocks types of variable age and composition (Anhaeusser 2006; Cawthorn et al. 2006; Robb et al. 2006). The craton hosts the Neoproterozoic Ventersdorp Supergroup and its temporal equivalents, which overlies the gold-bearing Witwatersrand Supergroup. The Ventersdorp Supergroup comprises the lowermost 2714 ± 8 Ma Klipriviersberg Group flood basalts, the unconformably overlying 2709 ± 4 Ma Platberg Group rift-fill sedimentary and bi-modal volcanic rocks and the uppermost 'Pniel Group', which comprises the sedimentary Bothaville Formation, and the volcanic Allanridge Formation. These near-coeval emplacement ages reported by Armstrong et al. (1991) on the Klipriviersberg and Platberg groups of the Ventersdorp Supergroup have implied that the Ventersdorp Supergroup constitutes a short-lived LIP. However, subsequent studies placed age constraints between ca. 2783 Ma (Wingate, 1998) and ca. 2730 Ma (de Kock et al., 2012) on the Klipriviersberg and Platberg group correlatives, hence challenging the 2714 ± 8 Ma age of the Klipriviersberg Group by Armstrong et al. (1991). Here we investigate two mafic sills intrusive into the Witwatersrand Supergroup successions, and examine their possibilities as feeders to the immediately overlying Klipriviersberg Group flood basalts. Baddeleyite grains within the dolerite sills were extracted and analysed using isotope dilution thermal ionization mass spectrometry (ID-TIMS) and complementary laser ablation inductively coupled plasma mass spectrometry (LA-ICP-MS).

The aims of this study are to: (1) evaluate the possibility of two mafic sills from the Witwatersrand sediments, belonging to a system of magmatic feeders to the overlying volcanic Klipriviersberg Group lavas (basal part of Ventersdorp Supergroup); (2) Test if LA-ICP-MS is feasible for U-Pb dating baddeleyite, compared to ID-TIMS U-Pb on baddeleyite.

2 Geological setting of the central Kaapvaal Craton

The Kaapvaal Craton (Fig. 1) in southern Africa preserves over 3600 million years of geological history, and it is one of the largest areas worldwide with well-

preserved Archean rocks (e.g., de Wit et al. 1992). The Kaapvaal Craton was formed and stabilized between 3.7 Ga and 2.7 Ga (e.g., de Wit et al., 1992), and thereafter followed deposition of sediments in large-scale basins on top of Archean greenstone belts and associated granitoids (Fig. 1). Today, basins include the lowermost and oldest Dominion Group, the Witwatersrand Supergroup, the Ventersdorp Supergroup, and the uppermost and youngest Transvaal Supergroup.

The Dominion Group occurs in the central part of the Kaapvaal Craton, and unconformably overlies the Archean granite-greenstone basement with a predominantly bi-modal volcanic succession (e.g., Marsh 2006). Sensitive High-Resolution Ion Microprobe (SHRIMP) U-Pb analyses of zircon from the Dominion Group yielded an age of 3074 ± 6 Ma (Armstrong et al. 1991). Unconformably covering the Dominion Group is the predominantly clastic Witwatersrand Supergroup, which comprises the lower West Rand Group and the upper Central Rand Group. The West Rand Group formed in a distal basin, hosting finer-grained sedimentary rocks, while the more proximal basin of the Central Rand Group comprises coarser-grained sedimentary rocks. The upper Central Rand Group contains gold-bearing quartz-pebble conglomerates which have been mined for gold for almost a century (Robb and Meyer 1995). These conglomerate-hosted gold ores are intruded by mafic dykes, which predominantly were emplaced along faults, presumably formed during the early development of the Ventersdorp Supergroup (Meier et al. 2009). Harris and Watkins (1990) showed that the mafic dykes have undergone metamorphism. Geochemical characteristics of the mafic dykes indicate that they are feeder dykes to the overlying flood basalts of the Klipriviersberg Group of the Ventersdorp Supergroup (Meier et al. 2009). Detrital zircons from the Orange Grove Formation in the West Rand Group yielded ages from 3330 to 2970 Ma (Robb and Meyer 1995). These detrital zircon ages indicate that the deposition of the Witwatersrand basin began at or after ca. 2970 Ma. The age of the upper West Rand is constrained by the 2914 ± 8 Ma age (Armstrong et al. 1991) of the Crown Member flood basalts, meaning that deposition of the West Rand occurred over a period of at least ca. 56 million years. The upper limit of the Witwatersrand Supergroup (Central Rand Group) sedimentation is not particularly well constrained, as it commenced sometime between 2714 ± 8 Ma (Armstrong et al. 1991), the age of the conformably overlying Klipriviersberg Group volcanic rocks, and ca. 2894 Ma (Robb and Meyer 1995), the age of detrital zircons from the Elfsburg Member conglomerates of the Witwatersrand

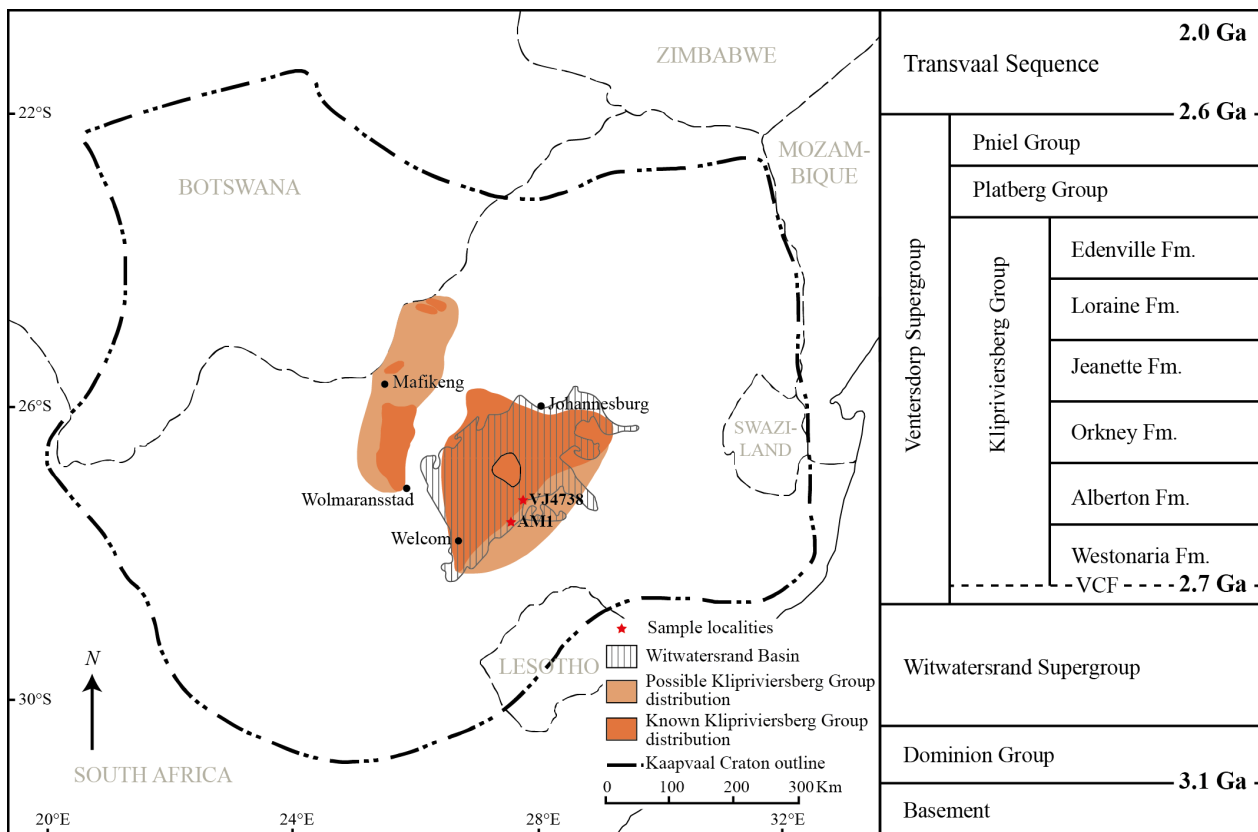


Figure 1. Simplified geological map showing the distribution of the Klipriviersberg Group rocks in South Africa in relation to the Witwatersrand Supergroup basin (modified after van der Westhuizen and de Bruijn, 2006) coupled with a general stratigraphic column of the Witwatersrand Supergroup (modified after Meier et al. 2009). The numbers to the right in the stratigraphic column are approximate ages in Giga-annum (Ga).

Supergroup. If the Witwatersrand Supergroup sedimentation ceased at ca. 2714 Ma, the basin would have been deposited over an interval of ca. 256 million years.

The third basin that developed on the Kaapvaal Craton was the Neoproterozoic volcano-sedimentary Ventersdorp Supergroup. The Ventersdorp Supergroup is the largest and most extensive Precambrian succession on the craton, and has been described as an intracratonic basin dominated by continental flood basalts, which were emplaced within north to northeast-trending graben structures (Burke et al. 1985; Marsh et al. 1992; Nelson et al. 1992). It mostly unconformably overlies the Witwatersrand Supergroup and the Archean basement, although towards the central part of the Kaapvaal Craton, the contact becomes conformable along the Klipriviersberg Group. The Ventersdorp Supergroup (Fig. 1) is subdivided into the lowermost Klipriviersberg Group, the overlying Platberg Group, and the uppermost Bothaville and Allanridge formations. The latter two are sometimes referred to as the ‘Pniel Group’. Unconformable relations are found between these three broad subdivisions (van der Westhuizen and de Bruijn 2006).

The Klipriviersberg Group at the base of the

Ventersdorp Supergroup mainly consists of flood basalts, and has a maximum thickness of approximately 1800 m in the centre of the Ventersdorp Basin (Fig. 1) (van der Westhuizen and de Bruijn 2006). The conformable contact between the Ventersdorp Supergroup and the underlying Witwatersrand Supergroup is defined by a horizon of conglomerates known as the Venterspost Conglomerate Formation (VCF) in the central Kaapvaal Craton. This formation constitutes the base of the Klipriviersberg Group (Bowen et al. 1986). In a study by Barton et al. (1990), detrital zircons from the base of the VCF were analysed, and a population at 2780 ± 5 Ma was recognized, which suggests that the VCF must have been deposited at or after this time. Hall and Els (2002) also found that the contact between the Klipriviersberg Group basalts and the VCF is conformable. The Klipriviersberg Group basalts exhibit an extraordinary lateral chemical homogeneity, which together with the lack of interbedded sedimentary rocks and erosional features, implies rapid emplacement and contemporaneous faulting (Crow and Condie 1988; van der Westhuizen and de Bruijn 2006). The basalts of the Klipriviersberg Group have been interpreted as being flood basalts derived from mafic feeder dykes and sills observed in the underlying

ing Witwatersrand Supergroup (Meier et al. 2009). The lowermost VCF is overlain by the extensive Westonia Formation, which consists of fine-grained basaltic and komatiitic flood basalts (Winter 1976). Although it has a wide lateral extent, it is only preserved in the deeper parts of the basin. Towards the basin margins the younger and overlying formations are onlapping, forming a structure where gradually younger formations form the base of the Klipriviersberg Group (van der Westhuizen and de Bruijn 2006). The Alberton, Orkney, Jeanette, Loraine and Edenville formations constitute almost exclusively volcanic rocks after the extrusion of the Westonia Formation. According to Crow and Condie (1988), these volcanic rocks show a gradually more primitive geochemical composition as the stratigraphic height increases. Armstrong et al. (1991) analysed zircons within the mafic flood basalts of the Alberton Formation and obtained a SHRIMP U–Pb age of 2714 ± 8 Ma, which was interpreted as the age of extrusion. However, when regarding the 2780 ± 5 Ma minimum age of the conformably underlying VCF, and the rapid extrusion of the flood basalts, the 2714 ± 8 Ma Klipriviersberg Group age was questioned by Wingate (1998) and de Kock et al. (2012). It was initially assumed that the lateral extent of the Klipriviersberg Group did not exceed the Witwatersrand Supergroup outcropping area and subsurface distribution. However, further mapping has indicated the presence of Klipriviersberg Group outliers, and the assumed possible distribution of the basaltic group now stretches far beyond the extent of the Witwatersrand Supergroup (Fig. 1) (van der Westhuizen and de Bruijn 2006).

The Platberg Group of the Ventersdorp Supergroup overlies the Klipriviersberg Group. The rocks of the Platberg Group were deposited during graben formation, and are found in isolated linear fault troughs (van der Westhuizen and de Bruijn 2006). A study by Armstrong et al. (1991) indicates an age of 2709 ± 4 Ma for quartz porphyries of the Makwassie Formation within the middle Platberg Group, which was interpreted as the crystallization age of the porphyritic rocks (interpreted as rhyolitic lava flows), and is the minimum age constraint for the unconformably underlying Klipriviersberg Group. Recent studies continue to identify contemporaneous rock units in different basins (e.g., the Hartswater Group of de Kock et al., 2012). The Hartswater Group outcrops on the western Kaapvaal craton (de Kock et al. 2012). It comprises the lower 2733 ± 3 Ma Mohle Formation and the upper 2724 ± 6 Ma Phokwane Formation (de Kock et al. 2012), and has traditionally, based on stratigraphic similarity, been considered a correlative of the $2709 \pm$

4 Ma Platberg Group (Armstrong et al. 1991). It has been suggested that the significant age difference between Platberg Group equivalents is a result of near-diachronous graben development across the Kaapvaal Craton, and that the Platberg Group equivalents were not deposited and/or extruded simultaneously in different basins (de Kock et al. 2012).

The uppermost part of the Ventersdorp Supergroup comprises the Bothaville and the Allanridge formations, which have also been known as the Pniel Group. The sedimentary Bothaville Formation unconformably overlies the Platberg Group. It predominantly comprises clastic sedimentary rocks which are upward fining in the stratigraphy, and are capped with dolomites (Bowen et al. 1986). The volcanic Allanridge Formation conformably overlies the Bothaville Formation. However, towards the margins of the Ventersdorp Supergroup, the relationship becomes unconformable. The rocks of the Allanridge Formation have been classified as basaltic andesite (van der Westhuizen and de Bruijn 2006).

3 Samples for U–Pb geochronology

Two mafic drill core samples, northeast of Welkom in South Africa in the vicinity of Kroonstad (Fig. 2), were selected for sampling using U–Pb geochronology on baddeleyite. Sample VJ4738 was obtained from a drill core located approximately 10 km north-east of Edenville, whereas sample AM1 was obtained from a drill core located approximately 10 km north of Steynsrus. Both mafic sills are situated within the Witwatersrand Supergroup succession immediately stratigraphically below the Klipriviersberg Group basalts at the base of the Ventersdorp Supergroup.

The drillcore near Steynsrus is approximately 3100 m long. The drillcore comprises the upper half of the West Rand Group (Tusschenin–Maraisburg formations) and the lowermost Central Rand Group (Blyvooruitzicht–Main formations) of the Witwatersrand Supergroup. AM1 represents an approximately 110 m thick mafic sill at a depth of approximately 1800 m, intruding into the Afrikaner Formation.

The Edenville drillcore is approximately 1700 m long, and comprises the Coronation–Babrosco formations of the West Rand Group. From this core, sample VJ4738 was obtained from an approximately 200 m thick dolerite sill at approximately 1400 m depth, intruding into the lowermost Palmietfontein Formation. Lithostratigraphic columns and sample depths are shown in Figure 2.

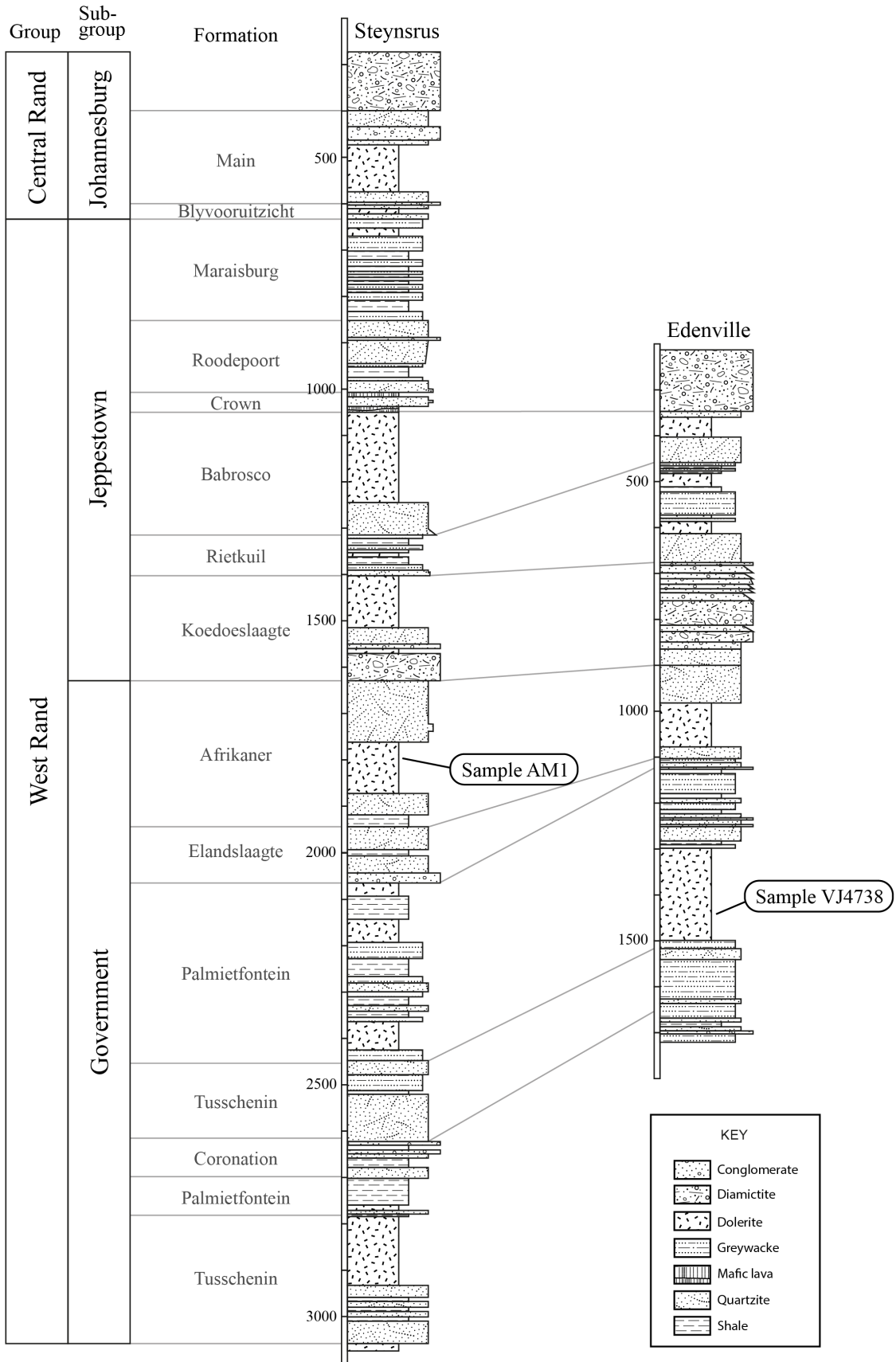


Figure 2. Lithostratigraphy of the Steynsrus and Edenville drill cores, and associated mafic sill sample depths. Note that sample AM1 was obtained stratigraphically higher than sample VJ4738. Depth intervals are shown in meters. Both drill cores are situated within the central Witwatersrand Supergroup.

4 Analytical protocols

4.1 Sample preparation

Mafic sill samples AM1 and VJ4738 were obtained from drill cores each weighing approximately 300 grams. The samples were crushed using a sledge hammer and thereafter grinded to a coarse powder using a swing mill. The powder was suspended with water and a drop of dish soap to reduce adhesive forces between particles. From the sample mixture, a small portion of approximately 30 grams was loaded onto a Wilfley water-shaking table. The extraction process was done according to the procedures presented by Söderlund and Johansson (2002).

From each sample only a small trace of the finest and most dense minerals were collected in a 5 L plastic bucket. As the minerals settled at the bottom of the bucket the excess water was removed. The mineral concentrate was carefully transferred into a glass petri dish in water. Magnetic minerals were then removed using a magnet, leaving mainly non-magnetic pyrite, baddeleyite and apatite. The baddeleyite was separated under a microscope and transferred to a new petri dish. From each sample the best-quality grains were selected for radiometric dating.

4.2 ID-TIMS

Fractions comprising one to five baddeleyite grains were transferred into pre-cleaned Teflon capsules using a hand-made plastic pipette. To minimize contamination and a high Pb blank, the grains were cleaned repeatedly by adding and removing 10–15 drops of 3.5 N nitric (HNO₃) acid. One of the cleaning steps included a 30 minute step on a hotplate at approximately 80° C. Following the cleaning step, 10 drops of concentrated hydrofluoric acid (HF), one drop of nitric acid and one drop of an isotopic tracer (²⁰⁵Pb–^{233–236}U) was added to each capsule. To ensure total homogenization of the Pb and U, from both the baddeleyite and the isotopic tracer, the capsules were placed in an oven at 190°C for three days. At the Laboratory for Isotope Geology, at the Swedish Museum of Natural History in Stockholm, the capsules were placed on a hotplate until the predominantly HF solution had evaporated. One drop of 0.25 N phosphoric acid (H₃PO₄) and 10 drops of ultrapure 6.2 N hydrochloric acid (HCl) were then added to each capsule, and dried down. The sample was then mixed into 2 µl Si-gel and placed on an outgassed Rhenium (Re) filament. The sample fractions were heated, by gradually increasing the current from 1 A to ca. 2.5 A, until the H₃PO₄ had burnt off and the samples turned white.

U and Pb were measured on a Finnigan Triton mass spectrometer (TIMS). As the filament temperatures approached approximately 1220–1260°C, the intensities of ²⁰⁴Pb, ²⁰⁵Pb, ²⁰⁶Pb, ²⁰⁷Pb and ²⁰⁸Pb were measured. The Pb-signal intensities were measured in either static mode with Faraday Cups (for high-intensity samples) or in dynamic mode with peak-switching using a Secondary Electron Multiplier (for low-intensity samples). The isotopes of ²³³U, ²³⁶U and ²³⁸U were measured as oxides at temperatures of approximately 1290–1340°C. Isotope dilution-thermal ionization mass spectrometry (ID-TIMS) data reduction was done using an “in-house” Microsoft Excel program. The program was made by Per-Olof Persson (Swedish Museum of Natural History in Stockholm) and based on the algorithms presented by Ludwig (2003). Isotope data was plotted and evaluated using ISOPLOT/EX 3.06 (Ludwig 2003). The uranium decay constants used were those reported by Jaffey et al. (1971). Initial common Pb was corrected for using the isotopic compositions from the model of Stacey and Kramers (1975). Error in ages and isotopic ratios are given at 2σ.

4.3 LA-ICP-MS

Due to the low yield of baddeleyite from AM1, only VJ4738 was chosen for laser ablation-inductively coupled plasma-mass spectrometry (LA-ICP-MS). Baddeleyite grains from sample VJ4738 were placed on double-sided adhesive tape, and casted into epoxy resin in a 2.5 cm wide by 0.5 cm high Teflon ring. After three days, the hardened epoxy mount was separated from the tape and polished for 20–140 seconds with 9, 3 and 1 µm diamond paste using a Struers rotopol automated polisher. The mount was subsequently cleaned with ethanol. The reference material used in the mount was baddeleyite from the 2059.60 ± 0.35 Ma Phalaborwa Complex (Heaman 2009).

The analyses were carried out at the newly established LA-ICP-MS laboratory in Lund, using a 193 nm Analyte G2 laser ablation unit with a two volume HelEx sample holder, and an Aurora Elite quadrupole ICP-MS. Ablation was done with a 5 Hz repetition rate, a fluence of approximately 4 j/cm², using 20 µm spot diameter. Detailed analytical conditions are presented in Appendix 1. The total acquisition time for each analysis was 55 seconds of which the first 20 seconds were used to determine the gas blank, followed by 28 seconds of laser ablation, and 7 seconds wash-out delay. The He carrier gas was mixed downstream with Ar before entering a “squid” signal smoothing device, made up of several tubes that split the stream before rejoining it into the single collector

quadrupole ICP-MS. The mass spectrometer was calibrated using NIST612 glass to give stable ^{206}Pb , ^{207}Pb and ^{238}U signals and low oxide production rates ($^{238}\text{U}^{16}\text{O}/^{238}\text{U}$ below 0.5 %) and a $^{232}\text{Th}/^{238}\text{U}$ ratio of approximately 1. ^{202}Hg , $^{204}(\text{Pb} + \text{Hg})$, ^{206}Pb , ^{207}Pb , ^{208}Pb , ^{232}Th , ^{235}U and ^{238}U intensities were determined through peak jumping. The interference of ^{204}Hg on ^{204}Pb was monitored by measuring ^{202}Hg assuming a $^{202}\text{Hg}/^{204}\text{Hg}$ ratio of 4.36 (natural abundance). Although ^{235}U were measured, the $^{207}\text{Pb}/^{235}\text{U}$ was calculated from the ^{238}U using $^{238}\text{U}/^{235}\text{U}=137.818$ following Hiess et al. (2012). The laser induced elemental fractionation and the instrumental mass bias on measured isotopic ratios was corrected for through standard-sample bracketing using the Phalaborwa standards (Heaman 2009). A total of 36 analyses were performed in the following order: 6 standards (Phalaborwa), followed by 7 unknown (VJ4738), 4 standards, 6 unknown, 4 standards, 5 unknown, and finally 4 standards. Data reduction was done using Iolite software (Paton et al. 2011) using the U–Pb geochronology DRS (data reduction scheme) routine of Paton et al. (2010). Correction routines for downhole fractionation and for instrumental drift were applied in the Iolite software. All isotope data was plotted and evaluated using ISOPLOT/EX 3.06 (Ludwig 2003). Analyses with an increased mass 204 count were rejected from the age calculation and no common lead correction was performed. Errors in ages are given at 2σ .

5 Results

The U and Pb ID-TIMS isotopic measurements are listed in Table 1, and data are plotted in a Wetherill concordia diagram in Figure 3 with grey and black ellipses representing VJ4738 and AM1, respectively. Baddeleyite grains extracted from sample VJ4738 were divided into four fractions. The grains have a distinct plate-like shape and are transparent with a light brown color, and their size is estimated to be less than 50 μm in the longest dimension. Regression

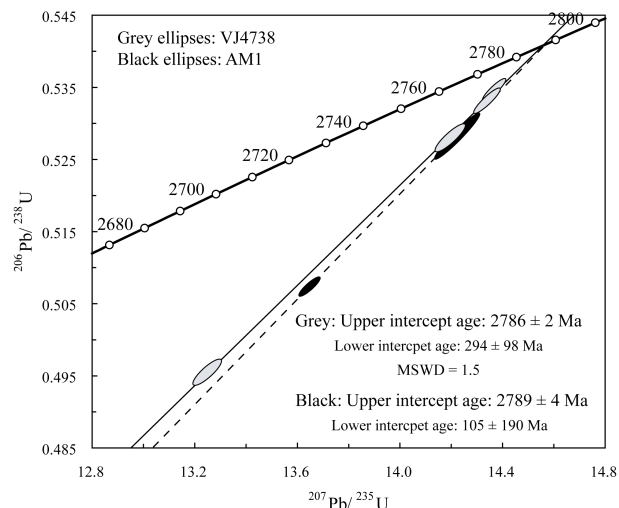


Figure 3. Wetherill concordia diagram for VJ4738 (grey ellipses) and AM1 (black ellipses). Data point error propagation ellipses are 2σ .

yields an upper intercept date of 2786 ± 2 Ma, and a lower intercept date of 294 ± 98 Ma, with a MSWD value of 1.5 (Fig. 3). The 2786 ± 2 Ma date is interpreted as the crystallization age of the VJ4738 mafic sill. A total of 12 baddeleyite grains were extracted from the core sample AM1 and split into two fractions. The grains are similar to VJ4738, do not show any sign of alteration, and are relatively transparent with a faint brown color. The two fractions yield a preliminary upper intercept date of 2789 ± 4 Ma, and a lower intercept date of 105 ± 190 Ma (Fig. 3). The 2789 ± 4 Ma date is identical within error with that of VJ4738, and is interpreted as the crystallization age of the AM1 mafic sill.

The $^{207}\text{Pb}/^{206}\text{Pb}$ dates and U–Pb isotopic data obtained from LA-ICP-MS is presented in Table 2 and plotted in a Wetherill concordia diagram in Figure 4a. Analytical results from the Phalaborwa standard material are presented in Appendix 2. No significant age difference was observed between analyses measured in the same sequence. There was however a significant difference in Pb, U and Th, which largely reflects different concentrations from grain to grain. The average

Table 1. U–Pb ID-TIMS data

Analysis no. (number of grains)	U/Th	Pbc/ Pbtot ¹⁾	$^{206}\text{Pb}/^{204}\text{Pb}$ raw ²⁾	$^{207}\text{Pb}/^{235}\text{U}$ [corr] ³⁾	$\pm 2\sigma$ % err	$^{206}\text{Pb}/^{238}\text{U}$	$\pm 2\sigma$ % err	$^{207}\text{Pb}/^{235}\text{U}$ [age, Ma]	$^{206}\text{Pb}/^{238}\text{U}$	$^{207}\text{Pb}/^{206}\text{Pb}$	$\pm 2\sigma$	Concordance
<i>Sample VJ-4738</i>												
Bd-1 (2 grains)	17.9	0.009	6783.5	14.3719	0.27	0.53472	0.24	2774.6	2761.3	2784.2	1.9	0.992
Bd-2 (3 grains)	14.6	0.009	6747.1	14.3443	0.30	0.53319	0.28	2772.8	2754.9	2785.8	2.1	0.989
Bd-3 (3 grains)	20.5	0.014	4403.1	14.2014	0.34	0.52804	0.30	2763.2	2733.2	2785.3	2.6	0.981
Bd-4 (2 grains)	25.0	0.019	3132.4	13.2505	0.34	0.49549	0.30	2697.7	2594.4	2776.0	2.9	0.935
<i>Sample AM-1</i>												
Bd-1 (6 grains)	4.9	0.025	2115.0	13.6500	0.25	0.50733	0.22	2725.7	2645.2	2786.0	1.9	0.949
Bd-2 (6 grains)	8.4	0.031	1906.0	14.2269	0.50	0.52824	0.50	2764.9	2734.0	2787.6	2.3	0.981

¹⁾ Pbc = common Pb; Pbtot = total Pb (radiogenic + blank + initial).

²⁾ measured ratio, corrected for fractionation and spike.

³⁾ isotopic ratios corrected for fractionation (0.1% per amu for Pb), spike contribution, blank (0.7 pg Pb and 0.07 pg U), and initial common Pb. Initial common Pb corrected with isotopic compositions from the model of Stacey and Kramers (1975) at the age of the sample.

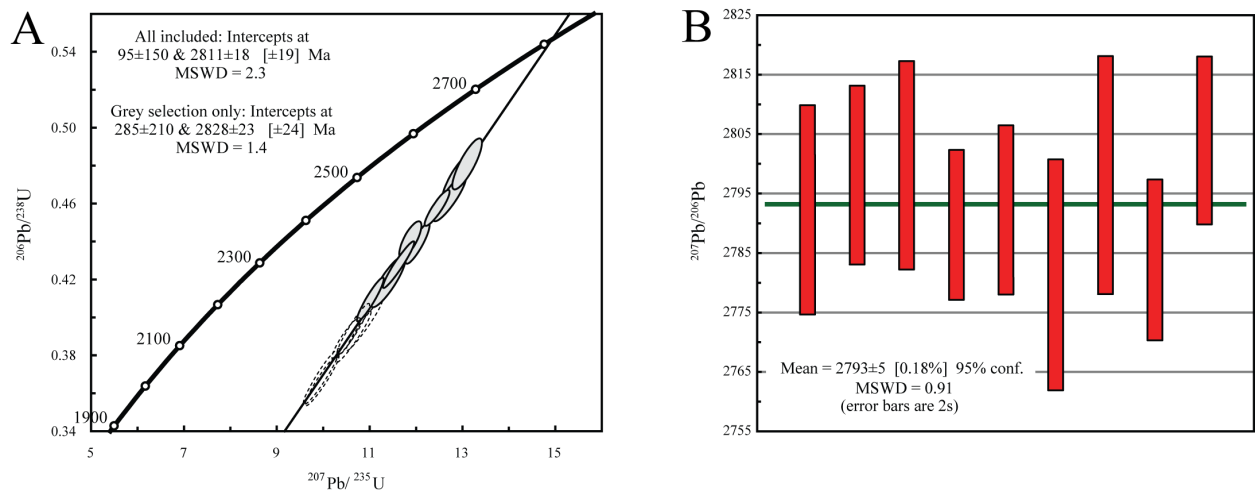


Figure 4. LA-ICP-MS Wetherill concordia diagram (A) for sample VJ4738 and its associated weighted average calculation (B) based on $^{207}\text{Pb}/^{206}\text{Pb}$ dates. The grey selection in the concordia diagram represents samples with $\geq 87\%$ concordance. Age uncertainties are given at 2σ .

mass-204 background signal was 1850 ± 12 counts per second (cps), 1860 ± 25 cps for the Phalaborwa (reference) material, and 1898 ± 31 cps for VJ4738. Assuming a detection limit of $10 \cdot \sigma$ of the blank, the content of ^{204}Pb could not be quantified. The signals did not display any significant increase in mass-204 signal during ablation, indicating an insignificant amount in initial Pb content. However, for a few analyses a rise in the 204 signal was recorded at the beginning of ablation, presumably reflecting surface contamination. A few analyses of VJ4738 displayed a small but significant increase in mass-204 with a corresponding increase in the $^{207}\text{Pb}/^{206}\text{Pb}$ ages (Table 2). These analyses were rejected from the age calculation. The remaining analyses from VJ4738 are plotted in a Wetherill concordia diagram. The analyses are variably discordant (between 83% and 94%), forming a discordant cluster. Using all analyses in the regression

yields an upper intercept date of 2811 ± 18 Ma and a lower intercept date at 95 ± 150 Ma, with a slightly elevated MSWD value of 2.3. Applying a locked lower intercept at 0 ± 100 Ma for the same data yields an upper intercept date at 2801 ± 7 Ma (MSWD=2.3). Excluding the six most discordant analyses ($\geq 14\%$ discordancy) (Fig. 4a), results in an upper intercept date of 2828 ± 23 Ma and a lower intercept date of 285 ± 210 Ma (MSWD=1.4). A forced regression at 0 ± 100 Ma yields an upper intercept date of 2800 ± 9 Ma (MSWD=2.1). A box-plot of the nine most concordant analyses ($\geq 87\%$ concordance) forms a coherent data set (Fig. 4b). A weighted mean of $^{207}\text{Pb}/^{206}\text{Pb}$ dates yield a date of 2793 ± 5 (MSWD=0.91). This result is in agreement with the VJ4738 ID-TIMS age of 2786 ± 2 Ma, and is associated with a MSWD value approaching unity, and is the preferred LA-ICP-MS crystallization age for this sample.

Table 2. LA-ICP-MS analytical results for sample VJ4738.

Analysis	Isotope ratios									Apparent ages (Ma)							
	$\frac{^{207}\text{Pb}}{^{235}\text{U}}$	$\pm 2\sigma$	$\frac{^{206}\text{Pb}}{^{238}\text{U}}$	$\pm 2\sigma$	Error corr.	$\frac{^{238}\text{U}}{^{206}\text{Pb}}$	$\pm 2\sigma$	$\frac{^{207}\text{Pb}}{^{206}\text{Pb}}$	$\pm 2\sigma$	Error corr.	$\frac{^{207}\text{Pb}}{^{235}\text{U}}$	$\pm 2\sigma$	$\frac{^{206}\text{Pb}}{^{238}\text{U}}$	$\pm 2\sigma$	$\frac{^{207}\text{Pb}}{^{206}\text{Pb}}$	$\pm 2\sigma$	Conc. (%)
VJ4738_0	12.860	0.250	0.474	0.010	0.855	2.111	0.043	0.196	0.002	0.265	2667	19	2495	43	2792	18	94
VJ4738_1	10.870	0.320	0.396	0.011	0.966	2.525	0.070	0.197	0.001	0.130	2503	27	2145	50	2799	12	86
VJ4738_2	12.020	0.210	0.439	0.009	0.877	2.278	0.045	0.197	0.002	0.456	2602	17	2343	39	2798	15	90
VJ4738_3	10.640	0.310	0.390	0.011	0.956	2.564	0.072	0.195	0.001	0.135	2483	27	2116	51	2787	12	85
VJ4738_4	12.710	0.290	0.463	0.010	0.883	2.160	0.047	0.197	0.002	0.219	2657	22	2449	45	2800	17	92
VJ4738_5	12.440	0.220	0.458	0.008	0.894	2.184	0.037	0.196	0.002	0.223	2632	16	2426	34	2790	13	92
VJ4738_6	11.380	0.310	0.419	0.011	0.869	2.387	0.063	0.196	0.002	0.252	2549	25	2248	51	2792	14	88
VJ4738_7	11.860	0.200	0.441	0.008	0.760	2.267	0.041	0.195	0.002	0.435	2590	15	2352	35	2781	19	91
VJ4738_8	13.090	0.260	0.481	0.011	0.827	2.079	0.048	0.197	0.002	0.438	2683	19	2530	48	2798	20	94
VJ4738_9	11.000	0.240	0.410	0.009	0.932	2.442	0.056	0.195	0.002	0.280	2518	21	2213	42	2784	13	88
VJ4738_10	9.940	0.320	0.369	0.012	0.947	2.710	0.088	0.196	0.002	0.080	2415	30	2017	54	2789	16	84
VJ4738_11	11.610	0.280	0.428	0.010	0.952	2.336	0.055	0.197	0.002	0.099	2566	24	2290	47	2804	14	89
VJ4738_12	10.480	0.250	0.389	0.009	0.903	2.571	0.059	0.196	0.002	0.061	2473	22	2114	41	2790	16	85
VJ4738_13	9.960	0.300	0.367	0.011	0.947	2.725	0.082	0.198	0.002	0.286	2423	27	2008	54	2808	16	83
VJ4738_14	10.630	0.290	0.394	0.011	0.943	2.538	0.071	0.196	0.002	0.196	2479	26	2132	50	2794	14	86
Reject204Pb_0	12.070	0.310	0.431	0.012	0.712	2.320	0.065	0.202	0.004	0.425	2605	24	2307	52	2844	32	89
Reject204Pb_2	10.310	0.400	0.357	0.013	0.958	2.801	0.102	0.207	0.002	-0.090	2450	36	1963	61	2883	18	80
Reject204Pb_3	5.800	0.450	0.209	0.016	0.976	4.785	0.366	0.200	0.003	0.011	1920	74	1217	86	2829	27	63

6 Discussion

6.1 LA-ICP-MS and ID-TIMS comparison on baddeleyite

There are several aspects to be considered when choosing between different U–Pb analytical techniques for dating of baddeleyite-bearing samples. A main advantage with ID-TIMS is the sensitivity of ID-TIMS data resulting in high precision (Kosler and Sylvester 2003). ID-TIMS requires the use of a calibrated tracer solution, which allows for accurate U/Pb age calculations. Additionally, common Pb corrections can be estimated accurately both for Pb blank, which is determined through blank runs, and initial Pb, with the isotopic compositions taken from the model of Stacey and Kramers (1975). Although ID-TIMS is generally referred to as the most reliable dating method, it also does have some important disadvantages. First, a significant amount of work must be made in a clean laboratory. Second, it is time-consuming, not just because of extensive laboratory work, but also due to the long running time at the mass spectrometer (2–3 hours per analysis), long preparation time, and use of ultra-clean chemicals. The last, but perhaps most critical disadvantage refers to the risk of mixing of magmatic and metamorphic age domains within a grain, although such complications are typically limited to altered and partly metamorphosed samples.

As opposed to ID-TIMS, the main advantage of the LA-ICP-MS is the high spatial resolution. LA-ICP-MS is a spot dating technique and hence allows for *in situ* U–Pb measurements of complex or simple grains. Thereby, younger domains, usually rims, can often be avoided and analysis can be restricted to primary magmatic volumes that escaped alteration. In addition, LA-ICP-MS is a relatively fast and affordable dating technique with just little sample preparation time required. However, LA-ICP-MS has much lesser sensitivity than ID-TIMS, and is associated with lower signal stability, hence leading to precision usually in excess of $\pm 1\%$ at 2σ for the age of the sample. Furthermore, an accurate common lead correction is almost impossible to obtain in single collector LA-ICP-MS studies because of the interference of ^{204}Hg , and the difficulty of estimating the proportion between the initial and common lead. The comparatively low sensitivity of the equipment adds to this problem. Consequently, the $^{207}\text{Pb}/^{206}\text{Pb}$ ages of uncorrected data tend to be too old for analyses with significant amounts of common Pb. An additional problem relates to the effect of downhole fractionation which occurs as uranium fractionates compared to lead. This means that the recorded $^{206}\text{Pb}/^{238}\text{U}$ and

$^{207}\text{Pb}/^{235}\text{U}$ ratios will vary during analysis, although it is usually feasible to make accurate corrections. The best way to minimize the analytical biases and increase the precision of LA-ICP-MS obtained data is through normalizing the raw data of the unknowns with a matrix matched standard (Wohlgemuth-Ueberwasser et al. 2015). Consequently, it may sometimes be difficult to evaluate the true concordance of LA-ICP-MS U–Pb data.

Regression of the U–Pb ID-TIMS data for VJ4738 yields an upper intercept crystallization age of 2786 ± 2 Ma (MSWD=1.5), which can be compared with the U–Pb ID-TIMS age of AM1, which yields a preliminary upper intercept crystallization age of 2789 ± 4 Ma. A weighted mean of the two U–Pb ID-TIMS ages yield a 2787 ± 2 Ma (MSWD=1.8) age and is within error of the LA-ICP-MS result, which gives a $^{207}\text{Pb}/^{206}\text{Pb}$ weighted mean crystallization age of 2793 ± 5 Ma (MSWD=0.91). Hence, both methods provide ages that marginally overlap within given 2σ uncertainties. Although it was possible to identify and reject LA-ICP-MS analyses with high common Pb content, the slightly increased $^{207}\text{Pb}/^{206}\text{Pb}$ age could be due to a few analyses having common Pb that could not be identified. This may explain why the mean of the LA-ICP-MS age is slightly older than the ID-TIMS age. These results indicate that the sills represent the same generation of mafic intrusions.

Although the upper intercept ages of VJ4738 and AM1 are identical, an interesting observation is the age difference of the lower intercept dates of 294 ± 98 Ma and 105 ± 190 Ma for VJ4738 and AM1, respectively. This difference suggests that discordance, presumably due to isotopic mixing, developed at different times and possibly by different causes. The younger date may relate to the emplacement of the extensive Karoo large igneous province, which was emplaced within a short period at ca. 180 Ma (e.g. Marsh et al. 1997). The older date is more difficult to link to a geological event but a combination of multiple events causing Pb-loss (e.g. during the ca. 1100 Ma Umkondo and the Karoo events) cannot be excluded. Notably there does not seem to be any isotopic disturbance related to shock metamorphism related to the Vredefort impact, dated at ca. 2023 Ma (Kamo et al. 1996).

The precision of the concordia ages obtained in this study is $\pm 0.1\%$ for the ID-TIMS ages and $\pm 0.2\%$ for the LA-ICP-MS age. The relatively high precision of the LA-ICP-MS data may be explained by the fact that it is an old sample which leads to high radiogenic Pb intensities and relatively high precision in the recorded $^{207}\text{Pb}/^{206}\text{Pb}$ ratio. Also, the high radiogenic Pb

content over the total Pb content makes common Pb correction less critical. In this study we could not utilize the LA-ICP-MS high-resolution capacity fully because the baddeleyite crystals were too small. Hence, we should expect the same degree of variability in discordance in LA-ICP-MS and ID-TIMS data, which is largely in agreement with the obtained data. The concordance of the ID-TIMS fractions is approximately 97%, whereas for the LA-ICP-MS analyses the average is approximately 91% (numbers restricted to the analyses included in the age calculation) and 88% (all analyses).

In conclusion, this study shows that the new LA-ICP-MS equipment at the Department of Geology, Lund University, offers a great opportunity for obtaining relatively precise and accurate single baddeleyite crystal $^{207}\text{Pb}/^{206}\text{Pb}$ ages for Neoproterozoic mafic intrusions.

6.2 Stratigraphy of the Neoproterozoic Ventersdorp Supergroup and its equivalents

We interpret that the 2787 ± 2 Ma age (the weighted mean of the two U–Pb TIMS ages) for the dolerite intrusions reported in this study to be the age of eruption for the Klipriviersberg Group flood basalts. Geological maps of the overturned stratigraphy of the Vredefort Dome show numerous mafic dykes cross-cutting the Witwatersrand Supergroup. However, these do not extend above into the stratigraphically overlying Klipriviersberg Group flood basalts. This suggests that the dolerite dykes and sills are feeders to the flood basalts themselves. Additionally, Meier et al. (2009) found that geochemical characteristics of mafic dykes and sills from the Witwatersrand Supergroup gold reefs matched those of the Klipriviersberg Group flood basalts. It is therefore reasonable to assume that the dolerite sills analysed in this study also belong to a system of dolerite intrusions that fed the overlying flood basalts, and that the obtained 2787 ± 2 Ma age is also the true age of the Klipriviersberg Group flood basalts. Furthermore, Barton et al. (1990) analysed detrital zircons from the base of the Ventersdorp Conglomerate Formation (VCF), which constitutes the base of the Klipriviersberg Group, and obtained a minimum age of 2780 ± 5 Ma. Considering a rapid extrusion of the flood basalts of the Klipriviersberg Group, a 2787 ± 2 Ma age would be in excellent agreement with the age of the conformably underlying VCF. Also, as discussed by de Kock et al. (2012), the 2734–2724 Ma Hartswater Group ages place reasonable doubt on the age of ca. 2714 Ma Klipriviersberg

Group as reported by Armstrong et al. (1991), which structurally has to be older than the overlying Platberg Group equivalents (which includes the Hartswater Group in a different basin equivalent of the Platberg Group). de Kock et al. (2012) suggests that the Klipriviersberg Group age reported by Armstrong et al. (1991) may be erroneous and significantly older. This hypothesis is strengthened by an angular unconformity between the nearly coeval Klipriviersberg and Platberg groups (Eriksson et al. 2002).

To address this issue, a reassessment of the Klipriviersberg Group data and its interpretation presented by Armstrong et al. (1991) is critical for the evaluation of the mafic intrusion ages reported in this study. Armstrong et al. (1991) applied a lower intercept forced through 0 Ma in their regression, hence assuming that the near-concordant analyses that cluster at ca. 1.1 Ga are erroneous. However, this assumption is questionable since the zircons may have formed during metamorphism, possibly associated with the 1.2–1.0 Ga Namaqua Orogeny (e.g. Cornell et al. 2006), and/or the emplacement of the ca. 1.1 Ga Umkondo Igneous Province (e.g., Hanson et al. 2004). This would explain the anhedral shape and concordant analysis of the zircons in this age group as reported by Armstrong et al. (1991). Armstrong et al. (1991) argued that the U–Pb systematics of the primary zircons, those that cluster concordant to near-concordant at 2.7 Ga, do not show any evidence of having ancient Pb-loss. As mentioned by Wingate (1998) however, it is reasonable to consider that the event which formed the younger generation of zircons may have affected the U–Pb systematics of the older generation of zircons. It may thus be relevant to reevaluate the data presented by Armstrong et al. (1991) using a locked lower intercept at approximately 1100 Ma. The Klipriviersberg Group sample EK-4/5 by Armstrong (1991), has in this study been re-evaluated using a 1.1 Ga lower intercept using ISOPLOT/EX 3.06 (Ludwig 2003). Ten analyses from sample EK-4/5 show $^{207}\text{Pb}/^{206}\text{Pb}$ dates significantly younger than 2.7 Ga. As described by Armstrong et al. (1991), they plot variably discordant with ages ranging from 2369 ± 35 Ma to 1764 ± 21 Ma. In addition there are a number of analyses that cluster at 1.0–1.1 Ga (see Figure 5). These analyses have been excluded from the Isoplot calculation. Additionally, the four most discordant analyses were removed from the 2.7 Ga near concordant to concordant data cluster. Using a locked lower intercept at 1100 ± 100 Ma, results in an upper intercept date of 2809 ± 45 Ma (MSWD=3.3) (Fig. 5). Another regression was performed excluding the oldest analysis described by Armstrong et al. (1991) as a xenocryst. With a locked

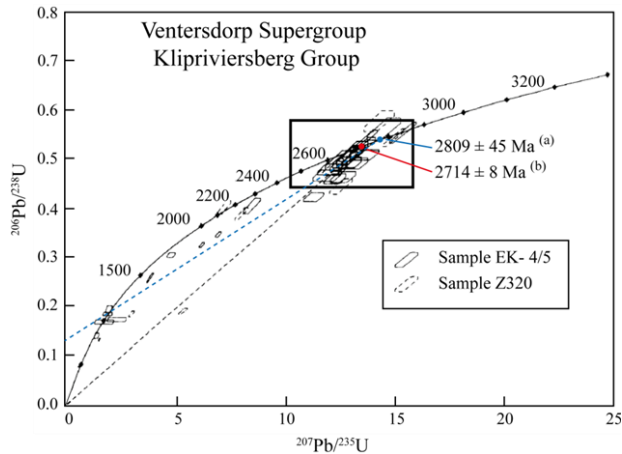


Figure 5. Wetherill concordia diagram showing Klipriviersberg Group basalt zircon analyses by Armstrong et al. (1991). A new age regression for sample EK-4/5, using analyses within the thick frame and a forced lower intercept at 1.1 Ga yields an upper intercept age of 2809 ± 45 Ma. Age references: (a) reevaluation in this study, and (b) Armstrong et al. (1991).

lower intercept at 1100 ± 100 Ma and data-point error ellipses at 2σ , this calculation yielded an upper intercept date of 2807 ± 48 Ma (MSWD=3.6). Notably, these new dates are in agreement with the 2787 ± 2 Ma dolerite intrusion age presented in this study.

The proposed 2787 ± 2 Ma Klipriviersberg Group age presented in this study solidifies the arguments discussed by Wingate (1998) and de Kock et al. (2012) for the ca. 2714 Ma age presented by Armstrong et al. (1991) on the Klipriviersberg Group basalts. This makes the Klipriviersberg Group significantly older than the overlying Platberg Group and Bothaville as well as the Allanridge formations (Fig. 6), and further demonstrated by the angular conformity observed between the Klipriviersberg and Platberg groups, and the age of the conformably underlying VCF.

Based on the significant age gap between the volcanic successions, we propose that the Ventersdorp Supergroup should be divided into two separate successions: one comprising the Klipriviersberg Group and another comprising the overlying Platberg Group, as well as the Bothaville and Allanridge formations.

In addition, there are now age equivalents of the Klipriviersberg Group basalts and its associated feeder system of dykes and sills on the Kaapvaal Craton. In the Amalia-Kraaipan granite-greenstone terrane, several granitoids overlap in age with the dolerite sills reported in this study (Fig 7 and Table 3). These include the Mosita, Mmathete and “red” granites. Similarly, the Turfloop granite in the northern Kaapvaal and the Gaborone-Kanye terrane have broadly coeval

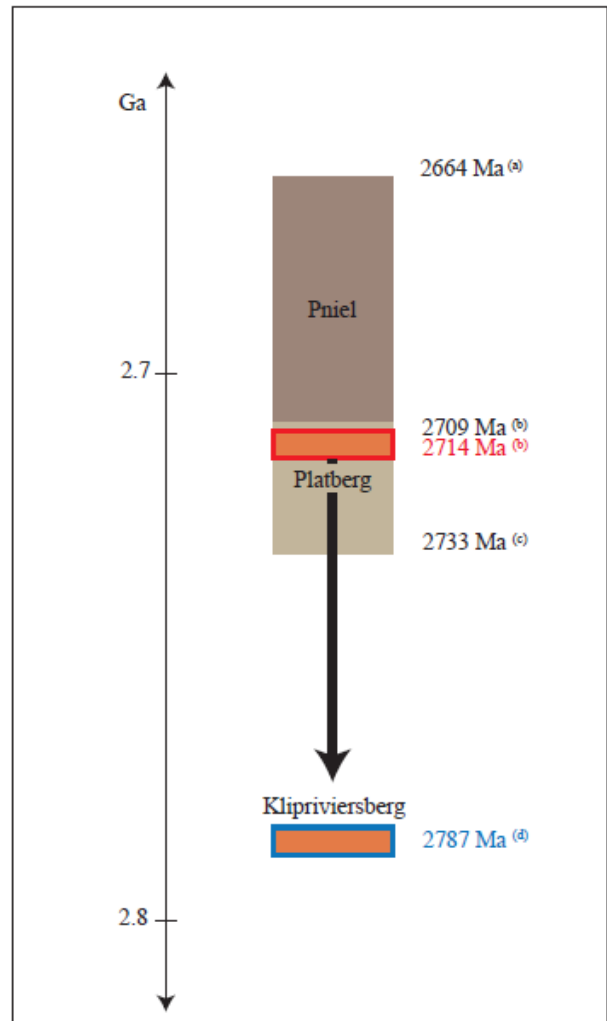


Figure 6. Schematic presentation of the geochronological development of the stratigraphic groups within the Ventersdorp Supergroup showing approximate ages of the geological units. The age of the Klipriviersberg Group would previously clash with the age of the stratigraphically unconformably overlying Platberg Group (Hartswater Group). However, the proposed Klipriviersberg Group age presented in this study addresses this problem. Age references: (a) Barton et al. (1990), (b) Armstrong et al. (1991), (c) de Kock et al. (2012), (d) this study.

ages. Near this area are also the Rooibokvlei granitoids in the Makoppa Dome and the Modipe Gabbro. Volcanic rocks in this area have also been reported with near coeval ages. This includes the Lobatse Volcanic Group and the Derdepoort Belt bimodal volcanic rocks. Similar cross correlations between the coeval rock units (Table 3) have previously been suggested by various authors (e.g., Grobler and Walraven 1993; Moore et al. 1993; Walraven et al. 1994; Walraven et al. 1996; Wingate 1998; Poujol et al. 2002; Anhaeusser and Poujol 2004; Mapeo et al. 2004; Robb et al. 2006; de Kock et al. 2012; Denyszyn et al. 2013; Ernst 2014).

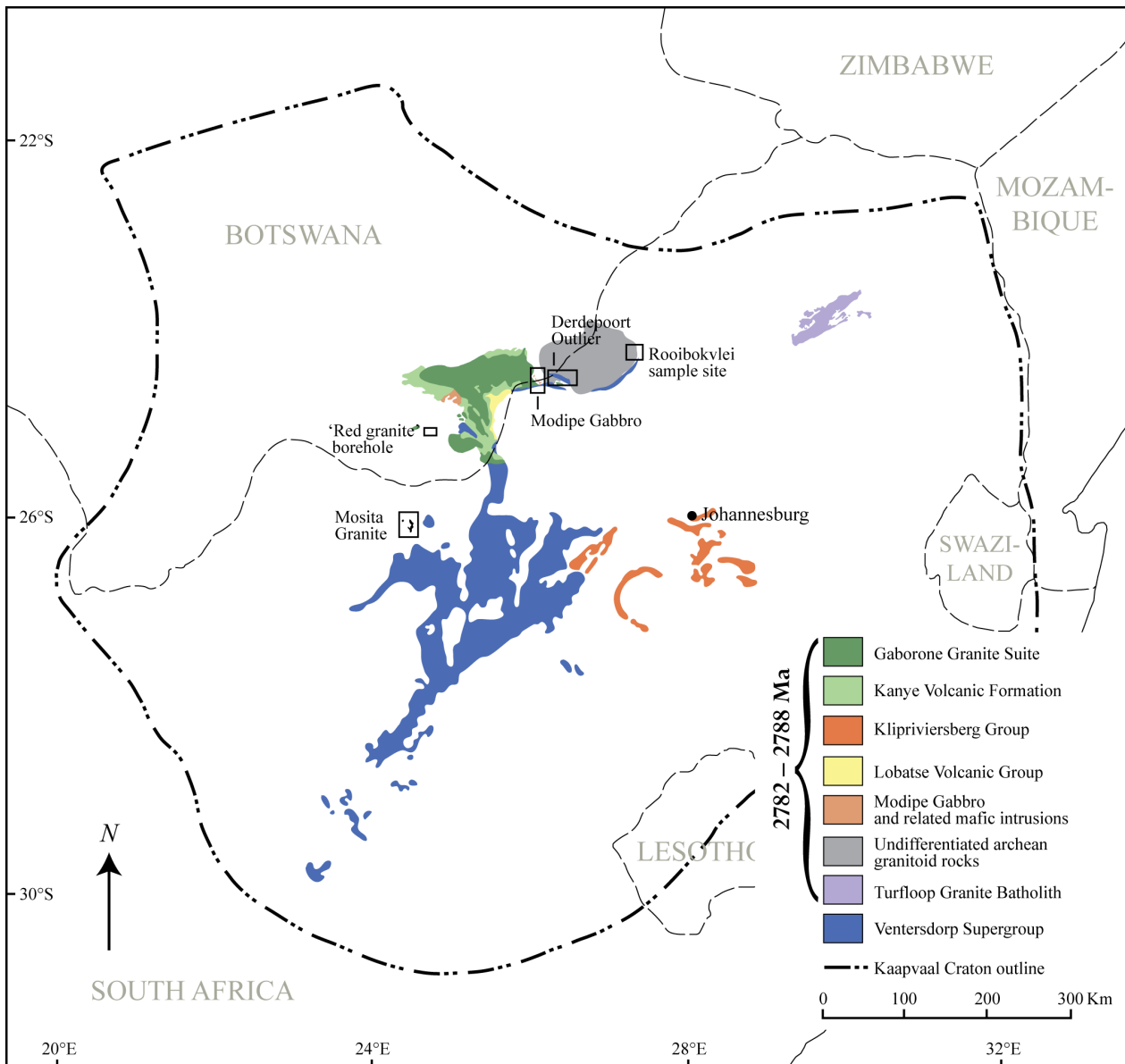


Figure 7. Outcrop distribution of early Neoproterozoic rocks on the central Kaapvaal Craton. Modified after van der Westhuizen and de Bruijn (2006), Ramotoroko et al. (2016) and Robb et al. (2006).

7 Implications

The 2787 ± 2 Ma mafic sills reported in this study cross-cut the gold-bearing Witwatersrand Supergroup successions, indicating that the placer gold deposits must predate the mafic feeders at 2787 ± 2 Ma. The new Klipriviersberg Group age also dates the end to the Witwatersrand Supergroup sedimentation at 2787 ± 2 Ma, indicating that the sediments were deposited within a maximum timespan of approximately 182 million years, as opposed to the previously suggested maximum timespan of 256 million years as suggested by the data by Armstrong et al. (1991).

We also propose that the coeval units (Table 3), which are all situated in the central Kaapvaal Craton

(Fig. 7), may indicate a major magmatic and volcanic event at ca. 2782–2788 Ma. The voluminous 10^5 km³ Klipriviersberg Group flood basalts and other bimodal magmatic events may qualify as a substantial Large Igneous Province (LIP) on the central part of the Kaapvaal Craton (van der Westhuizen and de Bruijn 2006; Ernst 2014). Additionally the 2787 ± 2 Ma age for the mafic sills reported in this study may imply that the Klipriviersberg Group basalts are equivalents of the Mount Roe Basalts of Australia and the Black Range dyke swarm (Wingate 1998; de Kock et al. 2009; Evans et al. 2017).

Table 3. Summary of U–Pb ages of intrusive early Neoproterozoic rocks on the Kaapvaal Craton.

Sample unit	Sample nature	Technique	Age, 2 σ (Ma)	Reference
Derdepoort Outlier				
Derdepoort Outlier	Basic lava	U–Pb TIMS, single-grain zircon	2769.3 \pm 4.6	Walraven et al. (1994)
Derdepoort Outlier	Porphyritic feldite	U–Pb SHRIMP, single-grain zircon	2781.1 \pm 4.4	Wingate (1998)
Gaborone Granite Suite				
Kgale Granite (north of Mafikeng)	Spherulitic microgranophyre	Pb–Pb zircon evaporation	2779.1 \pm 5.6	Grobler & Walraven (1993)
Kgale Granite (north of Mafikeng)	Granophyric granite	Pb–Pb zircon evaporation	2782 \pm 10	Grobler & Walraven (1993)
Kgale Granite (north of Mafikeng)	Granite	Pb–Pb zircon evaporation	2783.2 \pm 3.6	Grobler & Walraven (1993)
Gaborone Suite	Leucocratic granite	U–Pb ID TIMS, multi-grain zircon	2783.1 \pm 4.0	Moore et al. (1993)
Gaborone Suite	Granophyre	U–Pb ID TIMS, multi-grain zircon	2784.9 \pm 3.8	Moore et al. (1993)
Thamaga Granite (Kubung area)	A-type rapakivi granite	U–Pb, multiple zircon	2830 \pm 10 *	Sibiya (1988)
Kanye Volcanic Formation				
Kanye Formation	Rhyolite	Pb–Pb zircon evaporation	2783.9 \pm 8.8	Grobler & Walraven (1993)
Kanye Formation	Rhyolite	U–Pb ID TIMS, multi-grain zircon	2784.7 \pm 3.4	Moore et al. (1993)
Klipriviersberg Group				
Alberton Formation	Feldspar-phryic amygdaloidal lavas	U–Pb SHRIMP, single-grain zircon	2714 \pm 32	Armstrong et al. (1991)
'samples VJ4738 and AM1'	Dolerite	U–Pb ID-TIMS, baddeleyite	2787 \pm 2	THIS STUDY
Lobatse Volcanic Group				
Plantation Porphyry	Quartz porphyry	U–Pb TIMS, single-grain zircon	2781.7 \pm 1.9	Walraven et al. (1996)
Makoppa Dome				
Rooibokvlei Granitoid	Granodiorite/monzogranite	U–Pb ID-TIMS, single-grain zircon	2777 \pm 2	Anhaeusser and Poujol (2004)
Rooibokvlei Granitoid	Granodiorite/monzogranite	U–Pb ICP-MS	2777 \pm 35	Anhaeusser and Poujol (2004)
Rooibokvlei Granitoid	Granodiorite/monzogranite	U–Pb ID-TIMS, single-grain zircon	2797 \pm 2	Anhaeusser and Poujol (2004)
Mmatshete Granite				
Mmatshete Granite	Granite	Pb–Pb zircon evaporation	2775.2 \pm 7.4 *	Ref. in Mapeo et al. (2004)
Modipe Gabbro				
Modipe Gabbro	Gabbro	U–Pb ID-TIMS, baddeleyite	2784.0 \pm 1.0	Denyszyn et al. (2013)
Mosita Granite				
Mosita Granite	Adamellite	U–Pb, multiple zircon	2718 \pm 130	Burger & Walraven (1979)
Mosita Granite	Adamellite	U–Pb TIMS, single-grain zircon	2749 \pm 6	Anhaeusser & Walraven (1999)
Mosita Granite	Adamellite	U–Pb SHRIMP, zircon	2791 \pm 16	Poujol et al. (2002)
Red granite				
'red granite'	Granite	U–Pb SHRIMP, zircon	2781.6 \pm 11.2	Mapeo et al. (2004)
Turffloop Granite Batholith				
Turffloop Granite Batholith	Porphyritic granodiorite	U–Pb ID TIMS, multi-grain zircon	2.78 \pm 0.01 **	Henderson et al. (2000)

* Error unknown

** Age is given in Giga-annum (Ga)

8 Conclusions

Baddeleyite from two mafic sills hosted within the Witwatersrand Supergroup stratigraphy yield identical U–Pb ID-TIMS crystallization ages of 2786 ± 2 Ma and 2789 ± 4 Ma. The 2787 ± 2 Ma dolerite sill age presented in this study, together with previous geochronological and geochemical studies from the Ventersdorp Supergroup and its age equivalent sub-basins and from dykes cross-cutting the Witwatersrand Supergroup stratigraphy, indicate that the sills most likely acted as feeders to the overlying Klipriviersberg Group flood basalts at the base of the Ventersdorp Supergroup. This implies that the 2787 ± 2 Ma age obtained in this study is the true age of the Klipriviersberg Group basalts, i.e. significantly older than previous estimate.

The new 2787 ± 2 Ma age for the Klipriviersberg Group basalts implies a large temporal difference between the Klipriviersberg Group and the overlying 2709 ± 4 Ma Platberg Group. These two groups, both belonging to the Ventersdorp Supergroup, were previously considered part of the Ventersdorp LIP. The results presented in this study imply that the Klipriviersberg Group and coeval units may represent a separate LIP.

Complementary U–Pb LA-ICP-MS analysis of baddeleyites yielded a $^{207}\text{Pb}/^{206}\text{Pb}$ weighted mean crystallization age of 2793 ± 5 Ma. All dates overlap within error, and a 2787 ± 2 Ma (MSWD=1.8) age (the weighted mean of the two U–Pb TIMS ages) is interpreted as the emplacement age of the sills. The precision of the ages presented in this study is $\pm 0.1\%$ for the ID-TIMS upper intercept ages and $\pm 0.2\%$ for the LA-ICP-MS weighted mean age. This shows that the new LA-ICP-MS at the Department of Geology, Lund University, offers an opportunity for obtaining relatively precise and accurate single baddeleyite $^{207}\text{Pb}/^{206}\text{Pb}$ ages for Neoproterozoic intrusions.

9 Acknowledgements

First and foremost, I would like to express my gratitude to my main supervisor Prof. Ulf Söderlund for introducing me to this project, for helping me run the ID-TIMS, and for all the discussions, great advice and constructive criticism. Dr. Ashley Gumsley, thank you for lending me half your bookshelf and for helping me sort out the geological setting. Dr. Thomas Naeraa, thank you for helping me run the LA-ICP-MS and for the subsequent data reductions. I want to thank Prof. Michiel de Kock, from the Department of Geology at the University of Johannesburg, for providing me with

the samples and for making this thesis possible in the first place. I also want to thank Prof. Mike Hamilton from the University of Toronto for providing me with the front-page picture of this thesis. I would like to thank my fellow students for the laughs and fun that we have shared this past year, and an extra-big thanks to my fellow student Fisnik Balija for guidance on how to use Illustrator. Finally, I would like to thank my family for the love and support throughout all the past years of studies. Thank you all!

10 References

- Anhaeusser, C. R. 2006: Ultramafic and Mafic intrusions of the Kaapvaal Craton. In M. R. Johnson, C. R. Anhaeusser & R. J. Thomas (eds.): *The geology of South Africa*, 1 ed, 691. Geological Society of South Africa and Council for Geoscience
- Anhaeusser, C. R. & Pujol, M., 2004: Petrological, geochemical and U–Pb isotopic studies of Archaean granitoid rocks of the Makoppa Dome, northwest Limpopo Province, South Africa. *South African Journal of Geology* 107, 521–544.
- Anhaeusser, C. R. & Walraven, F., 1999: Episodic granitoid emplacement in the western Kaapvaal Craton: evidence from the Archæan Kraaipan granite-greenstone terrane, South Africa. *Journal of African Earth Sciences* 28, 289–309.
- Armstrong, R. A., Compston, W., Retief, E. A., Williams, I. S. & Welke, H. J., 1991: Zircon ion microprobe studies bearing on the age and evolution of the Witwatersrand triad. *Precambrian Research* 53, 243–266.
- Barton, E. S., Compston, W., Williams, I. S., Bristow, J. W., Hallbauer, D. K. & Smith, C. B., 1990: Provenance ages for the Witwatersrand Supergroup and the Ventersdorp Contact Reef; constraints from ion microprobe U–Pb ages of detrital zircons; reply. *Economic Geology and the Bulletin of the Society of Economic Geologists* 85, 1951–1952.
- Bowen, T. B., Marsh, J. S., Bowen, M. P. & Eales, H. V., 1986: Volcanic rocks of the Witwatersrand triad, South Africa. I: Description, classification and geochemical stratigraphy. *Precambrian Research* 31, 297–324.
- Burger, A. J. & Walraven, F., 1979: Summary of age determinations carried out during the period April 1977 to March 1978. *Annals of the Geological Survey of South Africa* 12, 209–218.
- Burke, K., Kidd, W. S. F. & Kusky, T., 1985: Is the Ventersdorp Rift System of Southern Africa related to a continental collision between the Kaapvaal and Zimbabwe Cratons at 2.64 Ga ago. *Tectonophysics* 115, 1–24.

- Cawthorn, R. G., Eales, H. V., Walraven, F., Uken, R. & Watkeys, M. K. 2006: The Bushveld Complex. In M. R. Johnson, C. R. Anhaeusser & R. J. Thomas (eds.): *The geology of South Africa*, 1 ed, 691. Geological Society of South Africa and Council for Geoscience
- Cornell, D. H., Thomas, R. J., Moen, H. F. G., Reid, D. L., Moore, J. M. & Gibson, R. L. 2006: The Namaqua-Natal Province In M. R. Johnson, C. R. Anhaeusser & R. J. Thomas (eds.): *The geology of South Africa*, 1 ed, 691. The Geological Society of South Africa.
- Crow, C. & Condie, K. C., 1988: Geochemistry and origin of late Archean volcanics from the ventersdorp supergroup, South Africa. *Precambrian Research* 42, 19–37.
- De Kock, M. O., Beukes, N. J. & Armstrong, R. A., 2012: New SHRIMP U–Pb zircon ages from the Hartswater Group, South Africa: Implications for correlations of the Neoproterozoic Ventersdorp Supergroup on the Kaapvaal craton and with the Fortescue Group on the Pilbara craton. *Precambrian Research* 204–205, 66–74.
- De Kock, M. O., Evans, D. a. D. & Beukes, N. J., 2009: Validating the existence of Vaalbara in the Neoproterozoic. *Precambrian Research* 174, 145–154.
- De Wit, M. J., Roering, C., Hart, R. J., Armstrong, R. A., De Ronde, C. E. J., Green, R. W. E., Tredoux, M., Peberdy, E. & Hart, R. A., 1992: Formation of an archaic continent. *Nature* 357, 553–562.
- Denyszyn, S. W., Feinberg, J. M., Renne, P. R. & Scott, G. R., 2013: Revisiting the age and paleomagnetism of the Modipe Gabbro of South Africa. *Precambrian Research* 238, 176–185.
- Eriksson, P. G., Condie, K. C., Van Der Westhuizen, W., Van Der Merwe, R., De Bruijn, H., Nelson, D. R., Altermann, W., Catuneanu, O., Bumby, A. J., Lindsay, J. & Cunningham, M. J., 2002: Late Archean superplume events: a Kaapvaal–Pilbara perspective. *Journal of Geodynamics* 34, 207–247.
- Ernst, R. E., 2014: *Large Igneous Provinces* Cambridge University Press, Cambridge, 653pp.
- Evans, D. a. D., Smirnov, A. V. & Gumsley, A. P., 2017: Paleomagnetism and U–Pb geochronology of the Black Range dykes, Pilbara Craton, Western Australia: a Neoproterozoic crossing of the polar circle. *Australian Journal of Earth Sciences* 64, 225–237.
- Grobler, D. F. & Walraven, F., 1993: Geochronology of Gaborone Granite Complex extensions in the area north of Mafeking, South Africa. *chemical Geology (Isotope Geoscience Section)* 105, 319–337.
- Hall, R. C. B. & Els, B. G., 2002: The origin and significance of load-induced deformation structures in soft-sediment and lava at the base of the Archean Ventersdorp Supergroup, South Africa. *Journal of African Earth Sciences* 35, 135–145.
- Hanson, R. E., Crowley, J. L., Bowring, S. A., Ramezani, J., Gose, W. A., Dalziel, I. W., Pancake, J. A., Seidel, E. K., Blenkinsop, T. G. & Mukwakwami, J., 2004: Coeval large-scale magmatism in the Kalahari and Laurentian cratons during Rodinia assembly. *Science* 304, 1126–1129.
- Harris, C. & Watkins, R. T., 1990: Fluid interaction in the Witwatersrand goldfields: Oxygen isotope geochemistry of Ventersdorp-age dolerite intrusions. *South African Journal of Geology* 93, 611–615.
- Heaman, L. M., 2009: The application of U–Pb geochronology to mafic, ultramafic and alkaline rocks: An evaluation of three mineral standards. *Chemical Geology* 261, 43–52.
- Henderson, D. R., Long, L. E. & Barton Jr., J. M., 2000: Isotopic ages and chemical and isotopic composition of the Archean Turfloop Batholith, Pietersburg granite-greenstone terrane, Kaapvaal Craton, South Africa. *South African Journal of Geology* 103, 38–46.
- Hiess, J., Condon, D. J., McLean, N. & Noble, S. R., 2012: $^{238}\text{U}/^{235}\text{U}$ systematics in terrestrial U-bearing minerals. In: science 335.
- Jaffey, A. H., Flynn, K. F., Glendenin, L. E., Bentley, W. C. & Essling, A. M., 1971: Precision Measurement of Half-Lives and Specific Activities of ^{235}U and ^{238}U . *Physical Review C* 4, 1889–1906.
- Kamo, S. L., Reimold, W. U., Krogh, T. E. & Colliston, W. P., 1996: A 2.023 Ga age for the Vredefort impact event and a first report of shock metamorphosed zircons in pseudotachylitic breccias and Granophyre. *Earth and Planetary Science Letters* 144, 369–387.
- Kosler, J. & Sylvester, P. J., 2003: Present Trends and the Future of Zircon in Geochronology: Laser Ablation ICPMS. *Reviews in Mineralogy and Geochemistry* 53, 243–275.
- Ludwig, K. R., 2003: User's Manual for Isoplot 3.00: A Geochronological Toolkit for Microsoft Excel. Berkeley, Berkeley Geochronology Center. 74 pp.
- Mapeo, R. B. M., Armstrong, R. A., Kampunzu, A. B. & Ramokate, L. V., 2004: SHRIMP U–Pb zircon ages of granitoids from the Western Domain of the Kaapvaal Craton, Southeastern Botswana: implications for crustal evolution. *South African Journal of Geology* 107, 159–172.
- Marsh, J. S. 2006: The Dominion Group In M. R. Johnson, C. R. Anhaeusser & R. J. Thomas (eds.): *The geology of South Africa*, 1 ed, 691. Geological Society of South Africa and Council for Geoscience

- Marsh, J. S., Bowen, M. P., Rogers, N. W. & Bowen, T. B., 1992: Petrogenesis of Late Archean Flood-Type Basic Lavas from the Klipriviersberg Group, Ventersdorp Supergroup, South Africa. *Journal of Petrology* 33, 817–847.
- Marsh, J. S., Hooper, P. R., Rehacek, J., Duncan, R. A. & Duncan, A. R. 1997: Stratigraphy and Age of Karoo Basalts of Lesotho and Implications for Correlations Within the Karoo Igneous Province. In J. J. Mahoney & M. Coffin (eds.): *Large Igneous Provinces*, 247–272 Geophysical Monograph.
- Meier, D. L., Heinrich, C. A. & Watts, M. A., 2009: Mafic dikes displacing Witwatersrand gold reefs: Evidence against metamorphic-hydrothermal ore formation. *Geology* 37, 607–610.
- Moore, M., Davis, D. W., Robb, L. J., Jackson, M. C. & Grobler, D. F., 1993: Archean rapakivi granite–anorthosite–rhyolite complex in the Witwatersrand Basin hinterland, southern Africa. *Geology* 21, 1031–1034.
- Nelson, D. R., Trendall, A. F., De Laeter, J. R., Grobler, N. J. & Fletcher, I. R., 1992: A comparative study of the geochemical and isotopic systematics of late Archaean flood basalts from the Pilbara and Kaapvaal Cratons. *Precambrian Research* 54, 231–256.
- Paton, C., Hellstrom, J., Paul, B., Woodhead, J. & Hergt, J., 2011: Iolite: Freeware for the visualisation and processing of mass spectrometric data. *Journal of Analytical Atomic Spectrometry* 26, 2508.
- Paton, C., Woodhead, J. D., Hellstrom, J. C., Hergt, J. M., Greig, A. & Maas, R., 2010: Improved laser ablation U–Pb zircon geochronology through robust downhole fractionation correction. *Geochemistry, Geophysics, Geosystems* 11, 1–36.
- Poujol, M., Anhaeusser, C. R. & Armstrong, R. A., 2002: Episodic granitoid emplacement in the Archaean Amalia–Kraaipan. *Journal of African Earth Sciences* 35, 147–161.
- Robb, L. J., Brandl, G., Anhaeusser, C. R. & Poujol, M. 2006: Archean Granitoid Intrusions. In M. R. Johnson, C. R. Anhaeusser & R. J. Thomas (eds.): *The geology of South Africa*, 1 ed, 691. Geological Society of South Africa and Council for Geoscience
- Robb, L. J. & Meyer, F. M., 1995: The Witwatersrand Basin, South Africa: Geological framework and mineralization processes. *Ore Geology Reviews* 10, 67–94.
- Sibiya, V. B., 1988: The Gaborone Granite Complex, Botswana, South Africa: an atypical rapakivi granite – massif anorthosite association. Amsterdam, Free University Press.
- Stacey, J. S. & Kramers, J. D., 1975: Approximation of terrestrial lead isotope evolution by a two-stage model. *Earth and Planetary Science Letters* 26, 207–221.
- Söderlund, U. & Johansson, L., 2002: A simple way to extract baddeleyite (ZrO₂). *Geochemistry, Geophysics, Geosystems* 3, 1–7.
- Walraven, F., Grobler, D. F. & Key, R. M., 1996: Age equivalence of the Plantation Porphyry and the Kanye Volcanic Formation, southeastern Botswana. *South African Journal of Geology* 99, 23–31.
- Walraven, F., Retief, E. A. & Moen, H. F. G., 1994: Single-zircon Pb-evaporation evidence for 2.77 Ga magmatism in northwestern Transvaal, South Africa. *South African Journal of Geology* 97, 107–113.
- Van Der Westhuizen, W. A. & De Bruijn, H. 2006: The Ventersdorp Supergroup. In M. R. Johnson, C. R. Anhaeusser & R. J. Thomas (eds.): *The Geology of South Africa*, 1 ed, 691. Geological Society of South Africa and Council for Geoscience.
- Wingate, M. T. D., 1998: A palaeomagnetic test of the Kaapvaal–Pilbara (Vaalbara) connection at 2.78 Ga. *South African Journal of Geology* 101, 257–274.
- Winter, H. D. L. R., 1976: A lithostratigraphic classification of the Ventersdorp succession. *Trans. Geol. Soc. S. Afr.* 79, 31–48.
- Wohlgenuth-Ueberwasser, C. C., Söderlund, U., Pease, V. & Nilsson, M. K. M., 2015: Quadrupole LA-ICP-MS U/Pb geochronology of baddeleyite single crystals. *Journal of Analytical Atomic Spectrometry*. 1191–1196 pp.

Appendix 1

LA-ICP-MS analytical conditions.

LA-ICP-MS	
<i>Laser ablation system</i>	
Make, model and type	Photon Machines, Analyte G2, excimer laser
Sample holder	HelEx2 Active 2-volume
Laser wavelength	193 nm
Pulse width	<4 ns
Fluence	4.06 J/cm ²
Repetition rate	5 Hz
Spot size	20 µm
Carrier gas	He (in LA) and He + Ar (in ICP-MS)
Background collection	20 seconds
Ablation duration	28 seconds
Wash-out delay	7 seconds
Cell carrier gas flow	ca. 1 l/min

<i>ICP-MS instrument</i>	
Make, model and type	Bruker, Aurora Elite, quadropole ICP-MS
Sample introduction	Via conventional tubing
RF power	1.4 kW
Sample gas flow	ca. 1.0 l/min Ar
Detection system	Single collector
Masses measured	202, 204, 206, 207, 208, 232, 235, 238
Intergration time per peak	40 ms on mass 207, 10 ms on all other masses
Total integration time per reading	119 ms

Appendix 2

LA-ICP-MS analytical results for the Phalaborwa standards.

Analysis	Isotope ratios										Apparent ages (Ma)						
	$\frac{^{207}\text{Pb}}{^{235}\text{U}}$	$\pm 2\sigma$	$\frac{^{206}\text{Pb}}{^{238}\text{U}}$	$\pm 2\sigma$	Error corr.	$\frac{^{238}\text{U}}{^{206}\text{Pb}}$	$\pm 2\sigma$	$\frac{^{207}\text{Pb}}{^{206}\text{Pb}}$	$\pm 2\sigma$	Error corr.	$\frac{^{207}\text{Pb}}{^{235}\text{U}}$	$\pm 2\sigma$	$\frac{^{206}\text{Pb}}{^{238}\text{U}}$	$\pm 2\sigma$	$\frac{^{207}\text{Pb}}{^{206}\text{Pb}}$	$\pm 2\sigma$	Conc. (%)
Phalaborwa_0	6.566	0.095	0.375	0.006	0.720	2.668	0.045	0.128	0.002	0.566	2053	13	2052	29	2068	22	100
Phalaborwa_1	6.551	0.091	0.372	0.006	0.706	2.685	0.040	0.128	0.001	0.455	2049	12	2038	26	2065	19	99
Phalaborwa_2	6.671	0.090	0.380	0.006	0.715	2.635	0.040	0.127	0.001	0.551	2065	12	2071	27	2057	19	100
Phalaborwa_3	6.629	0.097	0.378	0.006	0.758	2.648	0.040	0.126	0.001	0.379	2059	13	2063	26	2047	18	100
Phalaborwa_4	6.710	0.110	0.383	0.007	0.815	2.609	0.046	0.126	0.001	0.410	2070	15	2088	32	2043	18	101
Phalaborwa_5	6.606	0.095	0.377	0.007	0.806	2.656	0.047	0.127	0.001	0.524	2060	13	2056	31	2057	19	100
Phalaborwa_6	6.690	0.110	0.376	0.008	0.784	2.660	0.054	0.128	0.002	0.580	2067	15	2053	36	2076	22	99
Phalaborwa_7	6.590	0.098	0.376	0.006	0.713	2.662	0.043	0.127	0.002	0.490	2054	13	2056	28	2060	21	100
Phalaborwa_8	6.482	0.096	0.367	0.006	0.785	2.726	0.045	0.129	0.001	0.486	2042	13	2015	28	2078	18	99
Phalaborwa_9	6.526	0.087	0.376	0.006	0.728	2.657	0.040	0.126	0.001	0.449	2046	12	2056	26	2047	18	100
Phalaborwa_10	6.636	0.095	0.379	0.006	0.814	2.640	0.043	0.128	0.001	0.506	2061	13	2071	29	2067	17	100
Phalaborwa_11	6.452	0.089	0.366	0.005	0.775	2.736	0.040	0.128	0.001	0.494	2037	12	2006	26	2068	17	98
Phalaborwa_12	6.729	0.092	0.383	0.006	0.792	2.612	0.040	0.127	0.001	0.511	2074	12	2087	28	2058	17	101
Phalaborwa_13	6.713	0.097	0.383	0.006	0.797	2.608	0.041	0.127	0.001	0.411	2072	13	2089	28	2050	17	101

Tidigare skrifter i serien

”Examensarbeten i Geologi vid Lunds universitet”:

471. Malmgren, Johan, 2016: De mellankambriska oelandicuslagren på Öland - stratigrafi och facietyper. (15 hp)
472. Fouskopoulos Larsson, Anna, 2016: XRF-studie av sedimentära borrhärdar - en metodikstudie av programvarorna Q-spec och Tray-sum. (15 hp)
473. Jansson, Robin, 2016: Är ERT och Tidsdomän IP potentiella karteringsverktyg inom miljögeologi? (15 hp)
474. Heger, Katja, 2016: Makrofossilanalys av sediment från det tidig-holocena undervattenslandskapet vid Haväng, östra Skåne. (15 hp)
475. Swierz, Pia, 2016: Utvärdering av vattenkemisk data från Borgholm kommun och dess relation till geologiska förhållanden och markanvändning. (15 hp)
476. Mårdh, Joakim, 2016: WalkTEM-undersökning vid Revingehed provpumpningsanläggning. (15 hp)
477. Rydberg, Elaine, 2016: Gummigranulat - En litteraturstudie över miljö- och hälsopåverkan vid användandet av gummigranulat. (15 hp)
478. Björnfors, Mark, 2016: Kusterosion och äldre kustdyners morfologi i Skälderviken. (15 hp)
479. Ringholm, Martin, 2016: Klimatutlöst matbrist i tidiga medeltida Europa, en jämförande studie mellan historiska dokument och paleoklimatarkiv. (15 hp)
480. Teilmann, Kim, 2016: Paleomagnetic dating of a mysterious lake record from the Kerguelen archipelago by matching to paleomagnetic field models. (15 hp)
481. Schönström, Jonas, 2016: Resistivitet- och markradarmätning i Ängelholmsområdet - undersökning av korrosiva markstrukturer kring vattenledningar. (15 hp)
482. Martell, Josefin, 2016: A study of shock-metamorphic features in zircon from the Siljan impact structure, Sweden. (15 hp)
483. Rosvall, Markus, 2016: Spår av himlakroppskollisioner - bergarter i nedslagskratrar med fokus på Mien, Småland. (15 hp)
484. Olausson, My, 2016: Resistivitet- och IP-mätningar på den nedlagda deponin Gustavsfält i Halmstad. (30 hp)
485. Plan, Anders, 2016: Markradar- och resistivitetmätningar – undersökningar utav korrosionsförhöjande markegenskaper kring fjärrvärmeledningar i Ängelholm. (15 hp)
486. Jennerheim, Jessica, 2016: Evaluation of methods to characterise the geochemistry of limestone and its fracturing in connection to heating. (45 hp)
487. Olsson, Pontus, 2016: Ekologiskt vatten från Lilla Klåveröd: en riskinventering för skydd av grundvatten. (15 hp)
488. Henriksson, Oskar, 2016: The Dynamics of Beryllium 10 transport and deposition in lake sediments. (15 hp)
489. Brådenmark, Niklas, 2016: Lower to Middle Ordovician carbonate sedimentology and stratigraphy of the Pakri peninsula, north-western Estonia. (45 hp)
490. Karlsson, Michelle, 2016: Utvärdering av metoderna DCIP och CSIA för identifiering av nedbrytningszoner för klorerade lösningsmedel: En studie av Färgaren 3 i Kristianstad. (45 hp)
491. Elali, Mohammed, 2016: Flygsanddyners inre uppbyggnad – georadarundersökning. (15 hp)
492. Preis-Bergdahl, Daniel, 2016: Evaluation of DC Resistivity and Time-Domain IP Tomography for Bedrock Characterisation at Önnelöv, Southern Sweden. (45 hp)
493. Kristensson, Johan, 2016: Formation evaluation of the Jurassic Stø and Nordmela formations in exploration well 7220/8-1, Barents Sea, Norway. (45 hp)
494. Larsson, Måns, 2016: TEM investigation on Challapampa aquifer, Oruro Bolivia. (45 hp)
495. Nylén, Fredrik, 2017: Utvärdering av borrhålskartering avseende kalksten för industriella ändamål, File Hajdarbrottet, Slite, Gotland. (45 hp)
496. Mårdh, Joakim, 2017: A geophysical survey (TEM; ERT) of the Punata alluvial fan, Bolivia. (45 hp)
497. Skoglund, Wiktor, 2017: Provenansstudie av detritala zirkoner från ett guldförande alluvium vid Ravlunda skjutfält, Skåne. (15 hp)
498. Bergcrantz, Jacob, 2017: Ett fönster till Kattgatts förflutna genom analys av botenlevande foraminiferer. (15 hp)
499. O'Hare, Paschal, 2017: Multiradionuclide evidence for an extreme solar proton event around 2610 BP. (45 hp)
500. Goodship, Alastair, 2017: Dynamics of a

- retreating ice sheet: A LiDAR study in Värmland, SW Sweden. (45 hp)
501. Lindvall, Alma, 2017: Hur snabbt påverkas och nollställs luminiscenssignaler under naturliga ljusförhållanden? (15 hp)
502. Sköld, Carl, 2017: Analys av stabila isotoper med beräkning av blandningsförhållande i ett grundvattenmagasin i Älvkarleby-Skutskär. (15 hp)
503. Sällström, Oskar, 2017: Tolkning av geofysiska mätningar i hammarborrhål på södra Gotland. (15 hp)
504. Ahrenstedt, Viktor, 2017: Depositional history of the Neoproterozoic Visingsö Group, south-central Sweden. (15 hp)
505. Schou, Dagmar Juul, 2017: Geometry and faulting history of the Long Spur fault zone, Castle Hill Basin, New Zealand. (15 hp)
506. Andersson, Setina, 2017: Skalbarande marina organismer och petrografi av tidigcampanska sediment i Kristianstadsbassängen – implikationer på paleomiljö. (15 hp)
507. Kempengren, Henrik, 2017: Förorenings-spridning från kustnära deponi: Applicering av Landsim 2.5 för modellering av lakvattentransport till Östersjön. (15 hp)
508. Ekborg, Charlotte, 2017: En studie på samband mellan jordmekaniska egenskaper och hydrodynamiska processer när erosion påverkar släntstabiliteten vid ökad nederbörd. (15 hp)
509. Silvén, Björn, 2017: LiDARstudie av glaciala landformer sydväst om Söderåsen, Skåne, Sverige. (15 hp)
510. Rönning, Lydia, 2017: Ceratopsida dinosauriers migrationsmönster under krittiden baserat på paleobiogeografi och fylogeni. (15 hp)
511. Engleson, Kristina, 2017: Miljökonsekvensbeskrivning Revinge brunnsfält. (15 hp)
512. Ingered, Mimmi, 2017: U-Pb datering av zirkon från migmatitisk gnejs i Delsjöområdet, Idefjordenterrängen. (15 hp)
513. Kervall, Hanna, 2017: EGS - framtidens geotermiska system. (15 hp)
514. Walheim, Karin, 2017: Kvartsmineralogins betydelse för en lyckad luminiscensdatering. (15 hp)
515. Aldenius, Erik, 2017: Lunds Geotermisystem, en utvärdering av 30 års drift. (15 hp)
516. Aulin, Linda, 2017: Constraining the duration of eruptions of the Rangitoto volcano, New Zealand, using paleomagnetism. (15 hp)
517. Hydén, Christina Engberg, 2017: Drumlinerna i Löberöd - Spår efter flera isrörelseriktningar i mellersta Skåne. (15 hp)
518. Svantesson, Fredrik, 2017: Metodik för kartläggning och klassificering av erosion och släntstabilitet i vattendrag. (45 hp)
519. Stjern, Rebecka, 2017: Hur påverkas luminiscenssignaler från kvarts under laboratorieförhållanden? (15 hp)
520. Karlstedt, Filippa, 2017: P-T estimation of the metamorphism of gabbro to garnet amphibolite at Herrestad, Eastern Segment of the Sveconorwegian orogen. (45 hp)
521. Önnervik, Oscar, 2017: Ooider som naturliga arkiv för förändringar i havens geokemi och jordens klimat. (15 hp)
522. Nilsson, Hanna, 2017: Kartläggning av sand och naturgrus med hjälp av resistivitetmätning på Själland, Danmark. (15 hp)
523. Christensson, Lisa, 2017: Geofysisk undersökning av grundvattenskydd för planerad reservvattentäkt i Mjölkalånga, Hässleholms kommun. (15 hp)
524. Stamsnijder, Joaen, 2017: New geochronological constraints on the Klipriviersberg Group: defining a new Neoproterozoic large igneous province on the Kaapvaal Craton, South Africa. (45 hp)



LUNDS UNIVERSITET

Geologiska institutionen
Lunds universitet
Sölvegatan 12, 223 62 Lund